

Cardiac MRI: Recent Progress and Future Challenges

James P. Earls

INTRODUCTION

Few MR applications have held greater promise and encountered bigger challenges than cardiac imaging. The potential for cardiac MR imaging was recognized early, and many felt it could become the primary cardiac imaging modality. Research began in earnest with the development of whole body scanners and has continued unabated with Medline now listing over 5500 publications on the subject of cardiac MRI [1-7]. This enormous effort has proven that MR accurately depicts cardiac structure, function, perfusion, and myocardial viability with a capacity unmatched by any other single imaging modality. However, while it is an accepted and widely utilized tool for cardiovascular research, it is used infrequently in clinical practice, representing well less than 0.1% of all noninvasive cardiac imaging examinations performed in 1998 [8].

While the potential clinical impact of cardiac MR in patients with ischemic heart disease is great, specific techniques and capabilities have only recently become available outside of research centers. MR developments in cardiac morphology, function, myocardial perfusion and viability, and coronary angiography will be reviewed.

MORPHOLOGY

Accurate depiction of morphology is important in most cardiac applications. Numerous techniques have been developed to depict cardiac structure. These are generally referred to by the appearance of the intracardiac blood as "black blood" and "bright blood" techniques.

Black Blood Techniques

Spin-echo (SE) was the first sequence used for evaluating cardiac morphology. The development of ECG-gating made SE technique especially useful by substantially reducing motion artifacts [7,10]. SE sequences generally provide for good contrast between the myocardium and blood. These are called "black-blood" images because of the signal void created by flowing blood. Blood signal may appear brighter in slower flowing areas, such as immediately adjacent to the chamber wall. Presaturation with radiofrequency (RF) and reduction of the echo time (TE) minimizes blood signal and increases contrast on gated SE images [11]. Although widely

available, SE imaging has limited temporal resolution and is degraded by respiratory and other motion-related artifacts.

Shorter acquisition times are achieved with fast (or turbo) spin echo (FSE) pulse sequences, also known as rapid acquisition relaxation enhancement (RARE) [12]. Although faster, soft tissue contrast may be less optimal than with SE technique because of the wide range of acquired TEs inherent in FSE technique [13]. Numerous modifications to the basic FSE sequence have been made, including the use of one or more inversion pulses, increased echo train length, half-Fourier reconstruction, and

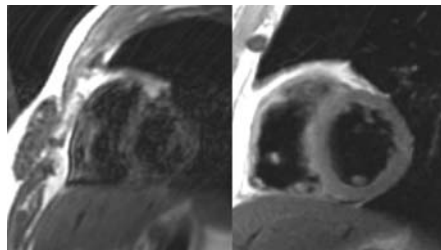


Fig. 1. Comparison of short-axis views at acquired with ECG-gated spin-echo (left) and T2-weighted double inversion recovery (DIR) imaging. Note that the ventricular blood signal is minimized and that the blood-myocardial interface is more clearly depicted on the DIR.

echo-planar techniques.

Single-shot FSE (SSFSE) sequences use a very long echo train in tandem with half-Fourier reconstruction [14]. The center of k space is acquired in a short time minimizing motion blurring. The rapid acquisition of multiple phase lines for a single TR allows for coverage of the entire heart in the timeframe of a single breathhold. SSFSE technique was reported to be a more rapidly acquired replacement for FSE in the evaluation of thoracic aortic disease, and it was proposed for cardiac use [15,16]. In cardiac imaging, the basic SSFSE technique has not proven useful because the long echo trains required coupled with the relatively short T2 leads to poor image contrast and blurring. However the SSFSE sequence can be modified for better cardiac results by reducing the echo train length, lowering the effective TE and using a blood-suppressed preparation method [17,18].

T2-weighted inversion recovery imaging is now used as the frontline sequence for depiction of cardiac morphology. This

technique uses a selective and a non-selective 180° inversion pulse followed by a long inversion time to null blood magnetization [19,20]. A second selective 180° inversion pulse can also be applied to null fat. This is referred to as double (or triple) inversion recovery (DIR, TIR respectively). The sequence is acquired either with breath hold or a non-breath hold technique and provides for excellent delineation of myocardial-blood interfaces (Figure 1). It effectively nulls blood and depicts blood-cardiac interfaces so well that the sequence has even been useful for performing coronary angiography [21].

Bright Blood Techniques

Bright blood imaging yields both morphologic and functional data. Blood generates bright signal intensity and multiple consecutive images are acquired that can be viewed dynamically to depict cardiac motion. Sequences include gradient-echo (GRE), fast GRE, segmented k-space fast GRE, and recently steady-state free precession (true FISP, FIESTA) techniques.

Gradient echo is well suited for cardiac imaging because of their short echo and repetition times. Blood appears bright compared to adjacent myocardium due to time-of-flight effects as well as the relatively long T2. Markedly turbulent blood loses signal due to intravoxel dephasing, a helpful artifact for assessing areas of stenosis or valvular regurgitation [22].

A segmented k-space approach provides high-resolution dynamic images of the heart that are acquired much more rapidly than prior techniques [23-25]. Using short echo times (2 msec) and short TRs (<10msec), multiple lines (segments) of k-space are acquired during each cardiac cycle. This is unlike prior GRE techniques where only a single line of k-space was acquired per cycle. Segmented k-space fast GRE imaging remains a mainstay for dynamic cardiac imaging and has been improved and adapted for even faster acquisition times [26-28]. However, the technique is limited by the need to maintain adequate enhancement of inflowing blood. At lower TRs now available with high-performance gradient systems, inflow enhancement of the cardiac blood pool diminishes and saturation occurs reducing myocardial-blood contrast. The inability to further reduce TR effectively limits achievable spatial and temporal resolution.

A new approach to improve cine imaging involves a technique known as steady-state free precession (SSFP). Image contrast in SSFP depends on the T1/T2 ratio of tissue and, unlike GRE techniques, is less dependent on flow. SSFP uses the available blood signal very efficiently and accurately depicts blood, myocardium, and epicardial fat [29]. First described in 1986, it was not used for cardiac applications for some years [30,31]. SSFP is susceptible to magnetic field inhomogeneities and requires very short TRs, limiting their use until recently. With magnetic field homogeneity improvements and development of higher performance gradient systems, diagnostic cardiac SSFP images are now obtained with limited artifacts [32-36]. This technique is also known as BFFE (balanced fast field echo), FIESTA (fast imaging employing steady-state acquisition), FISP (fast imaging with steady precession), and trueFISP.

SSFP sequences result in improved contrast between myocardium and ventricular cavities with clearer delineation of trabeculation and papillary muscles as compared to segmented k-space fast GRE techniques (Figure 2). The signal-to-noise (S/N) and contrast-to-noise (C/N) ratios of SSFP are substantially higher than conventional techniques [35-37]. Barkhausen et al found that the mean C/N ratio improved by an average of 46 % and 100% in short- and long-axis images, respectively compared with the standard cine gradient-echo sequences [37].

The reported C/N ratios are also higher than those obtained with contrast-enhanced gradient-echo techniques [38]. Pereles et al found that SSFP depicts morphologic and functional abnormalities with greater precision and provides greater diagnostic confidence than conventional techniques [36]. The other advantage of SSFP is improved temporal resolution [37,39].

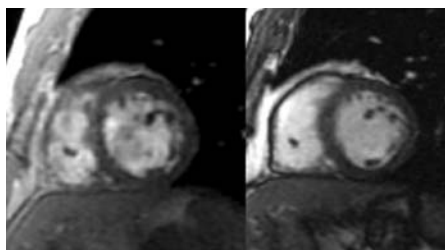


Fig. 2. Comparison of mid-diastolic short-axis views acquired with segmented k-space gradient echo imaging (left) and steady state free precession (SSFP)(right). Substantial blood pool heterogeneities are present in the segmented k-space gradient echo image (left) as compared with the homogeneous blood pool on the SSFP image (right). The SSFP technique has improved endocardial border definition throughout the cardiac cycle as compared with the older

Reduction in acquisition time by a factor of two to three at similar spatial resolutions is possible. Shorter acquisition times can also be exploited to improve spatial resolution.

CARDIAC FUNCTION

MR is well established for assessment of global and regional ventricular function. It allows accurate and reproducible quantification of ventricular volumes and masses, with the major advantage of not relying on potentially inaccurate ventricular geometry assumptions [40-43]. MR is regarded as the reference standard for determining ejection fraction (EF) and ventricular volumes [40,44,45]. Despite its proven research utility, cardiac function evaluation by MR has not attained widespread use in clinical practice due to its higher cost and longer times for image acquisition and analysis compared to echocardiography.

For measurement of global cardiac function, bright-blood cine MR has previously been performed in multiple short-axis views with a multi-phase, segmented k-space, gradient-echo sequence [46]. However, saturation in areas of low blood velocity reduces the contrast between ventricular cavity and myocardium on gradient echo images [47]. The saturation effect hampers endocardial contour detection with automatic or semi-automatic segmentation algorithms. This problem has been overcome with the introduction of the SSFP techniques.

As previously discussed, SSFP sequences recently became available for cardiac imaging and have improved C/N and shorter acquisition times compared with the cine GRE-techniques [30,34,42-44]. The performance of automatic contour detection algorithms for the endocardial contours and the interobserver variabilities have improved with SSFP technique [42,44]. However, the automatic contour detection algorithms did

not improve their performance for detection of epicardial contours and also had problems with artifacts due to off-resonance effects [42,44]. This underscores the fact that contour detection algorithms remain unreliable and further improvements are necessary. The implementation of SSFP sequences as a 3D data set obtained within a single breath-hold has been recently presented (Figure 3) [48,49].

Real-time techniques have been developed which continuously acquire images of the heart at sufficiently high rates and display them in a similar fashion as fluoroscopy [50,51]. The real-time techniques have fundamental advantages over conventional cardiac MR imaging by not requiring ECG-triggering, breath holding or navigator-echo gating. This reduces the setup time and duration of the exam, patient discomfort and associated cost [52]. It also enables imaging of patients with arrhythmias or severe heart disease, as well as performing stress testing faster.

To maintain a balance between high temporal and adequate spatial resolution, the frame-rate of real-time techniques must be increased along with the size of the acquisition matrix. The k-space area covered per unit time must grow as the inverse cube of pixel size. This presents a tremendous challenge to gradient performance and sequence design [53]. The combination of spoiled gradient-echo pulse sequences with multiecho, segmented EPI readouts have provided further improvement in scan time efficiency for use in real-time cine acquisition [27,28]. One hybrid sequences performed with a temporal resolution of ~60 ms has been used to obtain results of global function comparable to those with segmented k-space gradient echo techniques [54,55]. These sequences have been also implemented with multiecho rectilinear Cartesian [56,57] and radial k-space sampling schemes [58-60], with initial reports of good quality images and excellent spatial resolution relative to temporal resolution [45-55 ms].

Further increases of the acquisition speed can be achieved with reconstruction techniques such as sensitivity encoding (SENSE) and simultaneous acquisition of spatial harmonics (SMASH) [53,61]. Both reconstruct images using sensitivity information from multiple coil arrays. SENSE accelerates common breath-hold and real-time imaging by factors up to 3.2, and has been reported to obtain a temporal resolution down to 13 ms at a spatial resolution of 4.1mm [53]. Other recently developed but potentially promising reconstruction methods are the unaliasing by Fourier-encoding the overlaps using the

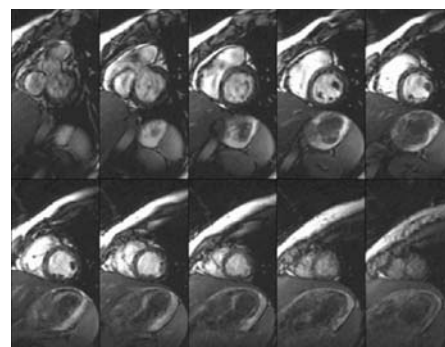


Fig. 3. Set of end-diastolic images obtained in a healthy volunteer with a cine 3D SSFP (FIESTA) sequence within a single breath-hold. The acquisition was acquired with a variable temporal k-space sampling scheme (VAST), a 256x192 matrix in a 34 cm FOV with 4 mm partitions.

temporal dimension (UNFOLD) and the selective line acquisition mode (SLAM) [62,63].

Ejection fraction (EF) is the most commonly used parameter of systolic function in clinical practice. However, it has limitations as a measurement of the contractile properties of the left ventricle. It is subject to error whether using a subjective visual estimate or a quantitative analysis as the endocardial borders may be traced inaccurately. EF is a global assessment of left ventricular performance and does not take into consideration regional contractile dysfunction, as commonly seen with ischemic heart disease and primary myocardial disease. The importance of regional contractile dysfunction is underscored by the fact that its extent and degree after myocardial infarction are important prognostic factors [64,65]. However, after decades of investigation there continues to be a clinical need for an objective and reproducible measurement of the regional myocardial contractile function [66].

Wall thickening is a useful measure of regional function and is more precise than wall motion analysis [67,68]. However, in the clinical setting this parameter is used with caution due to the heterogeneity of normal regional contraction and the wide range of thickening in normal and abnormal regions [69-71]. Wall thickening can be considered a measurement of radial strain. Strain is defined as the percent change in dimension from a resting state (end-diastole) to one achieved following application of a force (end-systole) [72]. Earlier animal studies proved the usefulness of strain analysis in assessment of regional contractile function [73]. Recently Götte et al showed that two-dimensional strain analysis from tagged MRI is more accurate in describing segmental function than wall thickening analysis, reporting a sensitivity of 92% and 69% and specificity of 99% and 92%, respectively in discriminating infarct-related dysfunctional myocardium from remote functional myocardium [74].

MR imaging is well established for assessment of global and regional ventricular function. Recently available SSFP sequences are more efficacious for functional analysis than prior techniques. In the future these may be replaced by enhanced real-time methods. Improved MR-tagging techniques and postprocessing methods for faster analysis have been developed and appear promising but have yet to be used on a widespread clinical basis.

MYOCARDIAL PERFUSION

Compromised myocardial perfusion (blood flow) is an indicator of possible reversible myocardial ischemia. The assessment of regional blood flow using MRI is best performed with dynamic imaging during the first pass of contrast media. Myocardium affected by a coronary artery lesion may not exhibit a perfusion deficit under resting conditions, but may not respond like a healthy vessel under stress. Consequently, the vascular resistance of a stenotic vessel is relatively high and results in a "vascular steal" phenomenon where increased flow is redirected to non-stenotic vessels, leading to an observable perfusion defect in the myocardial territory served by the stenotic vessel [87].

The physiology of passage of gadolinium chelates under normal and compromised blood flow determines the temporal resolution requirements of the imaging sequence. Gadolinium-chelates function as

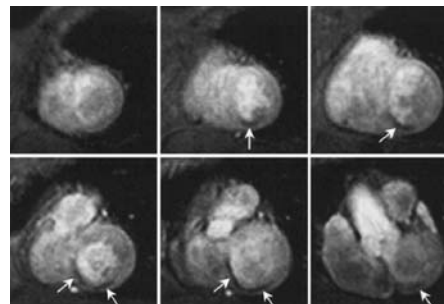


Fig. 4. Stress perfusion MR images depict six sections at one time point in a patient with 80% stenosis of the right coronary artery, as determined at conventional angiography. The region of perfusion deficit in the posterior septal wall (arrows) conforms to the vascular territory of the right coronary artery and does not appear in the rest images (not shown), indicating reversible ischemia.

an indicator of regional blood flow only in the first-pass phase; subsequent imaging results in artificial enhancement due to diffusion of contrast from adjacent regions with normal blood flow. Since the recirculation time of blood is between 5-15 seconds, perfusion imaging must image the first-pass passage of contrast material. First-pass perfusion defects alone represent both areas of reversibility and nonviable scar (Figure 4) [88-90].

Magnetic resonance remains an attractive tool for both the evaluation of reversible myocardial injury (ischemia) and for discrimination between salvageable tissue and irreversible injury. Depending on the acquisition technique chosen, qualitative examination of the MR perfusion data, quantitative analysis of myocardial perfusion

reserve, or both can be used for clinical evaluation of coronary artery disease.

MYOCARDIAL VIABILITY

Identification and differentiation of viable from non-viable myocardium plays a critical role in prognostication of patients with coronary artery disease. Until recently, Thallium SPECT and PET were the primary tools for this evaluation with dobutamine stress echocardiography fulfilling an ancillary but growing role. In the last few years, however, MRI has made a dramatic appearance in this arena with the introduction and rapid acceptance of the "delayed-enhancement" technique (DE-MRI) [106]. This imaging sequence identifies irreversible myocardial damage in both the acute and chronic settings, and combined with cine imaging can identify reversibly injured tissue that may benefit from revascularization.

The DE-MRI sequence is not the only MRI approach to myocardial viability, but has the greatest current acceptance. Other approaches include less effective variations on the gradient-echo DE-MRI technique [107]. Animal models demonstrated the potential for use of Manganese based contrast agents for differentiating viable from non-viable tissue. Manganese is a Ca^{++} analog actively taken up by viable myocardial cells. Viable tissue enhances on T1-weighted images, while non-viable tissue does not [108]. Manganese agents are not used in routine clinical cardiac imaging but may provide a potent alternative imaging method in the future. Sodium and potassium MRI is another efficacious tool for viability, but has seen little clinical use to date

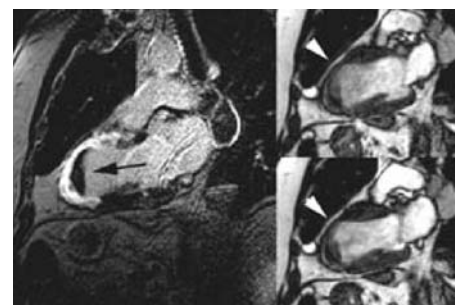


Fig. 5. 2D DE-MRI in a patient with chronic ischemic disease of the left anterior descending artery distribution. A two-chamber long axis image (left) reveals thinned tissue with transmural hyperenhancement involving the majority of the anterior wall, and entire apex, indicating a chronic transmural myocardial infarction. The left ventricular cavity is dilated and there is apical thrombus (black arrow). Cine images (right) at end-diastole (upper) and end-systole (lower) demonstrate akinesis of the anterior wall and apex (arrowhead).

because of the limited availability of multifrequency MRI scanners [109].

DE-MRI is performed following intravenous administration of gadolinium-chelate. After an appropriate delay (typically 10-20 minutes), breathhold inversion-recovery prepared, T1-weighted gradient-echo images are acquired. Viable myocardium is nulled via an iteratively chosen inversion delay time following the inversion pulse and data is acquired during an acquisition window of approximately 200 msec. or less. The result is an image where viable tissue is dark, and non-viable, fibrotic or scarred tissue has markedly increased signal intensity (Figure 5).

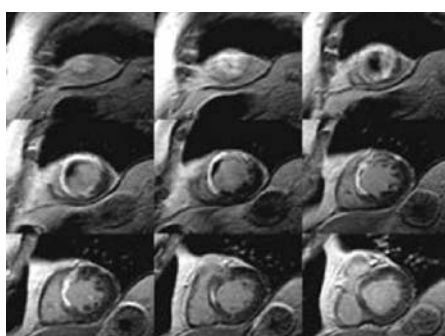


Fig. 6. 3D DE-MRI performed in a patient with a chronic infarction of the LAD distribution. This series of short axis images from apex to base was acquired in a single breathhold and has image quality nearly comparable to 2D images.

The imaging sequence typically used acquires 1 or 2 signal averages and has spatial resolution approximating 1.5 mm in-plane. The majority of published studies have evaluated myocardial viability using selected long axis images and a set of short axis images to encompass the left ventricle. This 2D approach requires multiple breath holds but can be accomplished in less than ten minutes. 3D approaches are recently being promoted as comparable in image quality and have the advantage of a single, albeit longer, breathhold to encompass the entire left ventricle (Figure 6).

DE-MRI has greater conspicuity of non-viable or infarcted tissue compared to spin-echo, steady-state free precession, and STIR techniques [110]. The precise mechanism of the differential contrast is not entirely clear, but data suggests that it reflects differing volumes of distribution. Non-viable tissue has substantial amounts of interstitial space, while viable tissue has little interstitial space. The “wash-in/out” rates for gadolinium-chelate in non-viable tissue are reduced, presumably because these processes are diffusion mediated. As a result, gadolinium-

chelate preferentially accumulates in irreversibly injured myocardium within minutes following contrast administration, and the enhancement lasts 45 minutes or longer [106,111, 112].

Assessment Of Chronic Myocardial Damage

Differentiating chronically damaged, infarcted myocardium from viable tissue using nuclear techniques is primarily a binary categorization as a result of the limited spatial resolution [113]. DE-MRI has substantially higher spatial resolution than nuclear techniques allowing for finer categorization of myocardial damage. The high-resolution images can detail the transmural extent of irreversibly damaged myocardium, and can depict separate small and large subendocardial infarctions from each other as well as from transmural damage [114,115].

DE-MRI is usually performed under rest conditions and combined with cine-MRI for wall motion information. Results are interpreted in one of three ways including: viable normal tissue (dark on viability images, normal wall motion); non-viable or irreversibly damaged tissue (bright on viability images, dysfunctional on cine imaging); and hibernating or “down-regulated” viable tissue (dark on viability imaging, dysfunctional on cine imaging).

The percentage of infarcted tissue per myocardial segment is inversely correlated with recovery of function following revascularization [116]. In a study by Kim et al. 42 patients were evaluated with viability imaging prior to revascularization, and with wall motion imaging both pre- and post-revascularization. Myocardial segments with little to no hyperenhancement in pre-revascularization viability imaging were highly likely to recover function. Conversely, myocardial segments with larger percentages of hyperenhancement were unlikely to recover function [117].

A further advantage of DE-MRI is the ability to visualize small, subendocardial areas of infarction that may be missed by nuclear techniques, including PET. Klein et al. compared DE-MRI to PET in patients with chronic ischemic cardiomyopathy and found a close correlation between the metabolic abnormalities on PET imaging and areas of hyperenhancement on DE-MRI [113]. Because of its higher spatial resolution, DE-MRI depicted hyperenhancing myocardium not identified by PET. The clinical significance of these regions is uncertain, but lends greater substance to DE-MRI as a technique for identifying myocardial abnormalities.

Assessment Of Acute Myocardial Damage

While DE-MRI has rapidly gained acceptance in the assessment of chronic ischemic disease, its role in the assessment of acute myocardial damage remains controversial. Some investigators suggest that the area of hyperenhancement on DE-MRI may be larger than the true area of necrosis and may include adjacent area at risk. The central issue to this debate is the time window during which imaging is performed [112]. Optimal agreement between pathologically proven irreversible damage and DE-MRI enhancement occurs 15-20 minutes following contrast administration [111,118]. Imaging earlier than this may overestimate the area of damage, while imaging later may underestimate lesion size, presumably because washout of contrast [119]. Further studies are needed to determine the optimal imaging window for accurate viability assessment.

Viability imaging provides insight into functional recovery following acute insults. Hillenbrand et al., studied dogs acutely with 45 minute, 90 minute, or permanent LAD occlusions and found a strong correlation between the severity of regional myocardial damage and duration of LAD occlusion. Perhaps more importantly, the transmural

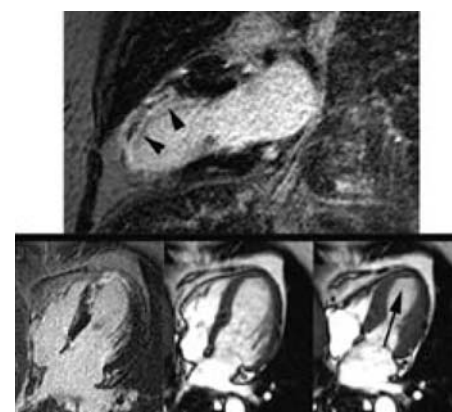


Fig. 7. DE-MRI in acute myocardial infarction. The lower images demonstrate DE-MRI (left) and cine images in end-diastole (middle) and end-systole (right). DE-MRI reveals transmural irreversible damage of the distal septum and apex, while the cine images reveal corresponding dysfunctional myocardium (arrow). The DE-MRI image in the upper row was performed in the two-chamber long axis projection and reveals transmural hyperenhancement of acute irreversible damage in the LAD distribution. Note the microvascular obstruction (‘no-reflow’ or focal non-hyperenhancing regions) in the subendocardium of the anterior wall (arrowheads) that is associated with greater post-infarction complications and poorer prognosis.

extent of damage found 3 days post-injury was most predictive of functional recovery on follow-up examinations performed 28 days after injury [120]. In another study by Fieno et al., imaging was performed in dogs subjected to acute injury. In both those with and without reperfusion DE-MRI differentiated viable from non-viable tissue during eight weeks of follow-up studies [121].

This predictive value of DE-MRI has been confirmed in humans. Choi et al. studied 24 patients with first AMI immediately following the acute event and then in follow-up. Regions of extensive enhancement were unlikely to recover function, while those with only mild damage had substantial recovery. Areas of dysfunctional myocardium with no enhancement in the peri-infarct zone were considered "stunned" and typically had recovery of function [122]. In addition to the areas of hyperenhancement reflecting acutely damaged, but perfused myocardium, DE-MRI also demonstrates myocardial zones of "no-reflow" or microvascular obstruction (Figure 7). As gadolinium-chelate cannot enter these regions they remain dark on DE-MRI images, but are surrounded by a rim of hyperenhancement [123,88]. Identifying the presence of microvascular obstruction is a strong prognostic marker for post-infarct complications and is better determined with DE-MRI than contrast-enhanced echocardiography [89,124,125].

DE-MRI is a sound technique for the assessment of myocardial viability in both the chronic and acute settings. Additional, large-scale studies are needed to precisely define the subsets of patients to gain the most benefit from such information. Further study is also needed to better characterize the significance of intermediate grades of non-transmural scar formation, where the predictive value of functional recovery following revascularization is less clear. Nonetheless, the capacity to assess viability under resting conditions without radiation exposure will no doubt rapidly increase the clinical use and acceptance of the technique and lead to wider dissemination.

CORONARY MRA

The coronary arteries have long been known to be one of the most difficult arterial circulations to image using MRI. The challenges for coronary magnetic resonance angiography (CMRA) are the inherent complex geometry and tortuosity of the coronary arteries, their small caliber (2-4 mm), and their continual displacement by respiratory and cardiac motion. Testimony to these difficulties has been the wide variety of

two-dimensional (2D) and three-dimensional (3D) CMRA techniques that have been investigated over the past decade. None have yet received universal acceptance, and invasive catheter x-ray angiography remains the primary diagnostic study for the clinical evaluation of coronary artery disease.

In this section, various CMRA techniques will be reviewed. Because EKG gating is employed by all methods to minimize cardiac motion effects on imaging, the methods are best categorized by the strategy employed for respiratory motion compensation: breath holding or navigator-echo gated acquisition. The newer techniques for contrast-enhanced CMRA will also be discussed.

Breath-hold techniques

In the early 1990's, Edelman et al. and Pennell et al. reported successful coronary illustration using a breath hold fat-suppressed fast two-dimensional (2D) gradient echo pulse sequence with a segmented k-space scheme [126-127]. A single image was obtained during each breath hold and imaging was targeted for diastole, when the heart was less mobile and coronary flow more brisk. Subsequent clinical assessments, however, revealed mixed success with sensitivities for the detection of hemodynamically significant stenoses ($\geq 50\%$ narrowing in arterial diameter) ranging from 63% to 90% [128-130].

Since that time, a number of improvements in gradient strength and pulse sequence design enabled faster and more efficient breath hold imaging. Meyer et al. introduced a spiral scanning which samples k-space in a spiral or curvilinear trajectory from the center of k-space out to the periphery [131]. The fat-suppressed 2D spiral gradient echo pulse sequence (Figure 8) provides a more efficient method for sampling k-space and enables improved spatial resolution (e.g. sub-millimeter in-plane resolution) and high arterial S/N compared to traditional 2D fast gradient echo acquisitions [132]. Faster scanning also enables the utilization of a larger portion of the R-R interval for systolic imaging and alternative multi-slice imaging algorithms [133,134].

Vessel tracking is one such newer algorithm that provides systolic as well as diastolic images [135,136]. The technique prescribes individual slice locations with the anticipated location of the coronary artery based on its location during the cardiac cycle. This 2D technique has improved scanning efficiency by a factor of three for any given breath hold

acquisition, minimizing the total number of breath holds required per examination.

Breath hold imaging has several inherent practical limitations [137]. Repetitive breath holds (e.g. 20-40) are often required for adequate anatomic coverage of the coronary arteries. Spatial registration between individual breath hold acquisitions is often poor and results in repeat acquisitions for sufficient anatomic coverage [138]. Patients with coronary artery disease poorly tolerate repetitive breath holds [139]. The short acquisition duration also limits spatial resolution. Breath holding is also not entirely static and some involuntary respiratory motion persists despite good patient cooperation and may result in arterial blurring [140].

Navigator-echo Techniques

The above stated breath hold limitations led to the development of respiratory-gated acquisitions, which enable imaging during tidal respiration. In 1989, Ehman and Felmlee described a novel technique for tracking of "view-to-view" tissue position using a "navigator" echo [141]. This technique can be used for prospective or retrospective gating of free-breathing CMRA [142-152]. Navigator-gating CMRA is typically performed using a fat-suppressed 3D gradient echo technique. Three-dimensional acquisitions are longer in duration but provide high spatial resolution volumetric data sets for improved depiction of the tortuous coronary arteries. Navigator echoes are placed over the right diaphragm for position detection and imaging is



Fig. 8. Breath-held multi-slice spiral images of the proximal coronary arteries from a single oblique axial acquisition in a healthy volunteer. Six images were acquired in mid-diastole in a 20 cm FOV with 2,048 data samples for each of the 20 spiral interleaves (2,048 x 20). Other scan parameters were 3.0 mm section thickness and 700 flip angle. Scan time was 17 seconds for a spatial resolution of 0.96 x 0.96 x 3.0 mm. A: Slice section illustrating the first 4-5 cm of the proximal right coronary artery. B: Slice section from the same acquisition showing the left main coronary artery, a proximal segment of the left anterior descending artery, and a first diagonal arterial branch

triggered for a 4-5 mm window. An end-expiration location is used for the navigator because it is sustained longer and more reliably during tidal respiration [146].

Patients better tolerate free-breathing navigator-echo gated acquisitions than breath hold acquisitions [139]. However, navigator-echo gated 3D CMRA yields lower quality images than breath hold 2D acquisitions because of image blurring of arterial edges despite successful navigator gating [153]. Navigator-gated images, nonetheless, are better than those of traditional respiratory gating using an external respiratory belt (respiratory “bellows”) [143,147]. However, navigator-echo gating is not always successful, especially in patients with irregular breathing patterns as may be seen in patients with an underlying pulmonary disease. Respiratory drift of diaphragm position outside of the trigger acceptance window for the navigator is another cause for failure [146]. This can be seen in patients who fall asleep during the imaging period or who are initially anxious during the beginning of scanning. Also, the long 10-15 minute exam times for a typical navigator-echo gated 3D CMRA are also more prone to bulk patient motion. The use of navigator-echo gating for 2D CMRA acquisitions (Figure 9) appears promising as its short (2-3 min) exam times remove many of the respiratory gating and image quality concerns of longer navigator-gated 3D acquisitions [154].

Paralleling the improvements in navigator echo implementation have been developments in 3D pulse sequence design for improvement of arterial depiction (i.e. arterial C/N) such as the use of a T2-weighted preparation prepulse [155-156]. In a multi-center study, Kim et al. recently reported very promising results using navigator-gated 3D CMRA using a T2-weighted preparation pre-pulse (and a fat-suppression pre-pulse) for illustration of the proximal 3-5 cm of the main coronary arteries [157]. Approximately 84% of the coronary arterial segments were sufficiently visualized (or “interpretable”) and 83% of clinically significant (≥ 50 percent reduction of diameter on x-ray angiography) were correctly detected. The mean 70-minute examination time unfortunately presents a number of logistical and patient-related problems for clinical implementation. Nonetheless, this study is noteworthy because it represents the first large multi-center evaluation of a CMRA technique. Prior clinical trials had been conducted primarily at a single institution and reproducibility of the technique not always universal.

Deshpande et al. recently reported another promising technique for improved coronary

arterial C/N that used a 3D magnetization-prepared SSFP technique [158]. This yielded significantly improved coronary arterial S/N (55%) and C/N (178%) when compared to a traditional fast gradient echo pulse

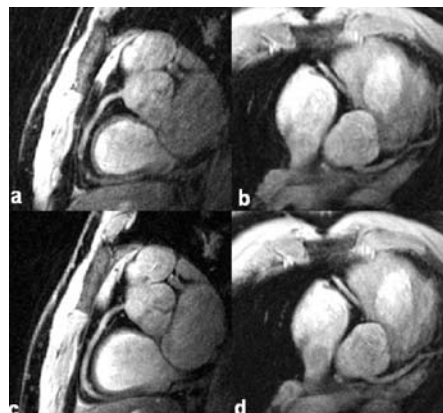


Fig. 9. Comparison between free breathing navigator-echo gated 2D spiral imaging (a and b) and breath-held multi-slice 2D spiral imaging (c and d). Image acquisition parameters for all images were 20 cm FOV, 3.0 mm section thickness, 2048 x 20 acquisition matrix, and 700 flip angle. This provided a spatial resolution of 0.96 x 0.96 x 3.0 mm for all images. Note that the quality of the free-breathing images (3 min scan time) was comparable to that of the breath-held images (19 sec scan time).

sequence. Coronary artery depiction is improved by the maintenance of steady-state transverse magnetization and the T2/T1 weighting of the pulse sequence that improves the blood-myocardial C/N.

Contrast-enhanced Techniques

The use of contrast media also increases C/N for CMRA [159-166]. Unlike the previously discussed techniques that rely principally on blood in-flow or T2/T1 differences, contrast-enhanced CMRA rely on T1 shortening by circulating contrast material. In-plane saturation, poor in-flow, and intra-voxel dephasing that can significantly hamper arterial depiction on non-contrast techniques are substantially less impeding to contrast-enhanced CMRA. These flow-related artifacts can result in the overestimation of arterial narrowing and are especially prevalent about stenoses where blood flow is turbulent and/or slow [130].

Contrast-enhanced CMRA methods have been developed for both traditional extracellular and newer blood-pool contrast agents (154-166). Techniques that use standard Gd-chelate contrast agents are designed for arterial phase imaging which is

achieved by the selective coordination of image acquisition (primarily the low spatial frequency data about the center of k-space) with peak enhancement of the coronary artery. Properly timed, coronary arterial C/N can be improved by 3 fold even when using a single 15 mL dose of Gd-chelate contrast agent [162]. The main limitation of extracellular contrast agents is their rapid leakage from the vascular space which results in background enhancement and diminished arterial C/N over time, thereby limiting the opportunities to perform repeated MRA or for the use of lengthy scans such as navigator-echo gated 3D CMRA.

Other contrast-enhanced CMRA techniques have been developed for blood pool contrast agents that have long persistence within the circulatory system. Blood pool contrast agents, like extracellular contrast agents, shorten the T1 of blood, and minimize the concerns related to flow-related image artifacts seen with non-contrast methods. Blood pool agents have much longer intravascular half-lives and provide prolonged arterial enhancement when compared with standard extracellular Gd-chelate contrast agents. They enable longer acquisition windows that can be used to achieve high spatial resolution coronary illustration and/or to perform repeated CMRA. Although still investigational, a variety of blood pool agents such as NC100150 (Amersham Imaging, Princeton, NJ) and MS-325 (EPIX Medical, Cambridge, MA) have shown promise for coronary artery illustration [163-166].

The challenges for coronary artery imaging have been multi-fold but progressive improvements continue to be made. Exam time, reliability, ease of use and education continue to be major practical issues that have impeded broad acceptance. Because of the technical challenges for achieving sufficient arterial C/N, spatial resolution and minimizing motion artifacts, coronary MRA techniques are continuing to undergo development and conventional x-ray angiography continues to be the only widely accepted method for clinical imaging of coronary artery stenosis. Because 20-40 percent of all diagnostic x-ray catheter angiograms reveal no clinically significant stenoses, the development of an accurate and robust CMRA technique would represent a significant improvement in the management of patients with suspected coronary artery disease [167].

CONCLUSION

As detailed above, there have been considerable technical and clinical advances in cardiac MR imaging within the

last several years. These advances include substantial overall improvements in temporal resolution, spatial resolution, motion and other artifact reduction, and improved depiction of contrast-enhancement for perfusion and viability analysis.

As MR has evolved, there also has been significant progress in the development of cardiac CT imaging, especially with the development of multi-detector array scanners (MDCT). The most promising cardiac CT application appears to be coronary CT angiography. While further validation is needed, two recent studies have had promising results. Nieman et al found 73% proximal and middle coronary segments assessable, and correctly diagnosed 81% of stenotic lesions within these vessels [168]. Achenbach et al reported an 85% sensitivity and 76% specificity for significant and a 91% sensitivity and 84% specificity for the absence of stenosis in assessable arteries [169]. While CT coronary angiography has had these initial promising results, other diagnostic cardiac applications are still in early stage of development.

While it is unclear which modality will win the race to become the preferred noninvasive coronary artery imaging modality, many other proven cardiac MR applications are available. Overall utilization of MR will likely continue to increase as techniques and other advances detailed in this report are disseminated clinically. Although the "one-stop-shop" for noninvasive cardiac diagnosis may not be available as soon as predicted, MR is an increasingly important tool for cardiovascular research and the clinical evaluation of patients with ischemic heart disease.

References

- [1] Higgins CB, Byrd BF 3rd, Farmer DW, Osaki L, Silverman NH, Cheitlin MD. Magnetic resonance imaging in patients with congenital heart disease. *Circulation* 1984 Nov;70(5):851-60
- [2] Ehman RL, McNamara MT, Pallack M, Hricak H, Higgins CB. Magnetic resonance imaging with respiratory gating: techniques and advantages. *AJR Am J Roentgenol* 1984 Dec;143(6):1175-82
- [3] Amparo EG, Higgins CB, Farmer D, Gamsu G, McNamara M. Gated MRI of cardiac and paracardiac masses: initial experience. *AJR Am J Roentgenol* 1984 Dec;143(6):1151-6
- [4] Choyke PL, Kressel HY, Reichel N, Axel L, Geffer W, Mamourian AC, Thickman D. Nongated cardiac magnetic resonance imaging: preliminary experience at 0.12 T. *AJR Am J Roentgenol* 1984 Dec;143(6):1143-50
- [5] McNamara MT, Higgins CB. Cardiovascular applications of magnetic resonance imaging. *Magn Reson Imaging* 1984;2(3):167-83
- [6] Lanzer P, Botvinick EH, Schiller NB, Crooks LE, Arakawa M, Kaufman L, Davis PL, Herfkens R, Lipton MJ, Higgins CB. Cardiac imaging using gated magnetic resonance. *Radiology* 1984 Jan;150(1):121-7
- [7] PUBMED (<http://www.ncbi.nlm.nih.gov>) search with MeSH terms (heart OR cardiac OR myocardium) AND (NMR OR nuclear magnetic resonance OR magnetic resonance imaging OR MRI).
- [8] Levin DC, Parker L, Sunshine JH, Pentecost MJ. Cardiovascular imaging: who does it and how important is it to the practice of radiology? *AJR Am J Roentgenol* 2002 Feb;178(2):303-6
- [9] Higgins CB, Editor; Special Issue: Cardiovascular MRI, *JMRI* 1999; 10(5):589-899.
- [10] Stark DD, Higgins CB, Lanzer P, Lipton MJ, Schiller N, Crooks LE, Botvinick EB, Kaufman L. Magnetic resonance imaging of the pericardium: normal and pathologic findings. *Radiology*. 1984 Feb;150(2):469-74.
- [11] Pettigrew RI. Dynamic cardiac MR imaging. Techniques and applications. *Radiol Clin North Am* 1989 Nov;27(6):1183-203
- [12] Haddad JL, Rofsky NM, Ambrosino MM, Naidich DP, Weinreb JC. T2-weighted MR imaging of the chest: comparison of electrocardiograph-triggered conventional and turbo spin-echo and nontriggered turbo spin-echo sequences. *J Magn Reson Imaging* 1995; 5:325-329
- [13] Pettigrew RI, Oshinski JN, Chatzimavroudis G, Dixon WT. MRI techniques for cardiovascular imaging. *J Magn Reson Imaging* 1999 Nov;10(5):590-601
- [14] Semelka RC, Kelekis NL, Thomasson D, Brown MA, Laub GA. HASTE MR imaging: description of technique and preliminary results in the abdomen. *J Magn Reson Imaging* 1996; 6:698-699.
- [15] Stererman DH, Krinsky GA, Lee VS, Johnson G, Yang BM, Rofsky NM. Thoracic aorta: rapid black-blood MR imaging with half-Fourier rapid acquisition with relaxation enhancement with or without electrocardiographic triggering. *Radiology* 1999; 213:185-191
- [16] Stehling MK, Holzknicht NG, Laub G, Bohm D, von Smekal A, Reiser M. Single-shot T1- and T2-weighted magnetic resonance imaging of the heart with black blood: preliminary experience. *MAGMA* 1996 Sep-Dec;4(3-4):231-40
- [17] Vignaux OB, Augui J, Coste J, Argaud C, Le Roux P, Carlier PG, Duboc D, Legmann. Comparison of single-shot fast spin-echo and conventional spin-echo sequences for MR imaging of the heart: initial experience. *Radiology* 2001 May;219(2):545-50
- [18] Le Roux P, Gilles RJ, McKinnon CG, Carlier P. Optimized outer volume suppression for single-shot fast spin echo cardiac imaging. *J Magn Reson Imaging* 1998; 8:1022-1032
- [19] Edelman RR, Chien D, Kim D. Fast selective black-blood MR imaging. *Radiology* 1991; 181:655-660.
- [20] Simonetti OP, Finn JP, Withe RD, Laub G, Henry DA. "Black blood" T2-weighted inversion recovery MR imaging of the heart. *Radiology* 1996; 199:49-57
- [21] Stuber M, Botnar RM, Kissinger KV, Manning WJ. Free-breathing black-blood coronary MR angiography: initial results. *Radiology* 2001 Apr;219(1):278-83
- [22] Utz JA, Herfkens RJ, Heinsimer JA, Shimakawa A, Glover G, Pelc N. Valvular regurgitation: dynamic MR imaging. *Radiology* 1988 Jul;168(1):91-4
- [23] Atkinson DJ, Edelman RR. Cineangiography of the heart in a single breath hold with a segmented turboFLASH sequence. *Radiology* 1991 Feb;178(2):357-60
- [24] Edelman RR, Wallner B, Singer A, et al. Segmented turbo FLASH: method for breath-hold MR imaging of the liver with flexible contrast. *Radiology* 1990; 177:515-521.
- [25] Chien D, Atkinson D, Edelman RR. Strategies to improve contrast in turboFLASH imaging: reordered phase encoding and k-space segmentation. *J Magn Reson Imaging* 1991; 1:63-70
- [26] Leung DA, Debatin JF, Wildermuth S, McKinnon GC, von Schulthess GK. Cardiac imaging: comparison of two-shot echo-planar imaging with fast segmented k-space and conventional gradient-echo cine acquisitions. *J Magn Reson Imaging*. 1995 Nov-Dec;5(6):684-8.
- [27] Reeder SB, Atalar E, Farnesh AZ, McVeigh ER. Multi-echo segmented k-space imaging: an optimized hybrid sequence for ultrafast cardiac imaging. *Magn Reson Med* 1999; 41:375-385.
- [28] Epstein FH, Wolff SD, Arai AE. Segmented k-space fast cardiac imaging using an echo-train readout. *Magn Reson Med* 1999; 41:609-613.
- [29] Zur Y, Wood ML, Neuringer LJ. Motion-insensitive, steady-state free precession imaging. *Magn Reson Med* 1990;16:444-459
- [30] Oppelt A, Graumann R, Barfu H, et al. FISP - a new fast MRI sequence. *Electromedica* 1986;54:15-18.
- [31] Haacke EM, Wielopolski PA, Tkach JA, Modic MT. Steady-state free precession imaging in the presence of motion: application for improved visualization of the cerebrospinal fluid. *Radiology* 1990; 175: 545-552
- [32] Haacke EM, Tkach JA. Fast MR imaging: techniques and clinical applications. *Am J Radiol* 1990; 5: 951-964.
- [33] Deimling M, Heid O. Magnetization prepared True FISP imaging (Abstract). In: Proceedings of the 2nd Annual Meeting of ISMRM, San Francisco, 1994. p 495
- [34] Bundy J, Simonetti O, Laub G, Finn JP. Segmented TrueFISP cine imaging of the heart (abstract). In: Proceedings of the 7th Annual Meeting of the ISMRM, Philadelphia, 1999: p.1282.
- [35] Fang W, Pereles FS, Bundy J, et al. Evaluating LV function using real-time True FISP: a comparison with conventional MR techniques (Abstract). In: Proceedings of the 8th Annual Meeting of ISMRM, Denver, 2000. p 308
- [36] Pereles FS, Kapoor V, Carr JC, Simonetti OP, Krupinski EA, Baskaran V, Finn JP. Usefulness of segmented trueFISP cardiac pulse sequence in evaluation of congenital and acquired adult cardiac abnormalities. *AJR Am J Roentgenol* 2001 Nov;177(5):1155-60
- [37] Barkhausen J, Ruehm SG, Goyen M, et al. MR evaluation of ventricular function: true fast imaging with steady-state precession versus fast low-angle shot cine MR imaging: feasibility study. *Radiology* 2001; 219:264-269.
- [38] Stillman AE, Wilke N, Jerosch-Herold M. Use of an intravascular T1 contrast agent to improve MR cine myocardial-blood pool definition in man. *J Magn Reson Imaging* 1997;7:765-767.
- [39] Plein S, Bloomer TN, Ridgway JP, et al. Steady-state free precession magnetic resonance imaging of the heart: comparison with segmented k-space gradient-echo imaging. *J Magn Reson Imaging* 2001;14:230-236.

- [40] Pattynama PM, De Roos A, Van der Wall EE, Van Voorthuisen AE. Evaluation of cardiac function with magnetic resonance imaging. *Am Heart J* 1994;128:595-607
- [41] Sakuma H, Fujita N, Foo TK, et al. Evaluation of left ventricular volume and mass with breath-hold cine MR imaging. *Radiology* 1993;188:377-380
- [42] Bloomgarden DC, Fayad ZA, Ferrari VA, et al. Global cardiac function using fast breath-hold MRI: validation of new acquisition and analysis techniques. *Mag Reson Med* 1997; 37:683-692.
- [43] Heusch A, Koch JA, Krogmann ON, et al. Volumetric analysis of the right and left ventricle in a porcine heart model: comparison of three-dimensional echocardiography, magnetic resonance imaging and angiocardiology. *Eur J Ultrasound* 1999;9:245-55.
- [44] Tadamura E, Kudoh T, Motooka M, et al. Assessment of regional and global left ventricular function by reinjection TI-201 and rest Tc-99m sestamibi ECG-gated SPECT: comparison with three-dimensional magnetic resonance imaging. *J Am Coll Cardiol* 1999; 33:99
- [45] Vaduganathan P, He ZX, Vick GW, et al. Evaluation of left ventricular wall motion, volumes, and ejection fraction by gated myocardial tomography with technetium 99m-labeled tetrofosmin: a comparison with cine magnetic resonance imaging. *J Nucl Cardiol* 1999; 7:31-56.
- [46] Bluemke DA, Boxermann JL, Atalar E, McVeigh ER. Segmented k-space cine breath-hold cardiovascular imaging. I: Principles and technique. *AJR Am J Roentgenol* 1997; 169:395-400.
- [47] Chien D, Edelman RR. Ultrafast imaging using gradient echoes. *Magn Reson Q* 1991; 7:31-56.
- [48] Foo TKF, Ho VB, Kraitchman D. Single breath-hold single-phase and CINE 3D acquisition using variable temporal k-space sampling (abstract). In: Proceedings of the 9th Annual Meeting of the ISMRM, Glasgow 2001:112.
- [49] Scheffler K. 3D cardiac cine imaging in a single breath-hold using elliptically reordered 3D trueFISP (abstract). In: Proceedings of the 9th Annual Meeting of the ISMRM, Glasgow 2001: 113.
- [50] Rzedizan RR, Pykett IL. Instant images of the human heart using a new, whole-body MR imaging system. *AJR Am J Roentgenol* 1987;149:245-250.
- [51] Matthaei D, Haase A, Henrich D, Dühmke E. Cardiac and vascular imaging with an MR snapshot technique. *Radiology* 1990;177:527-532.
- [52] Yang PC, Kerr AB, Liu AC, et al. New real-time interactive cardiac magnetic resonance imaging system complements echocardiography. *J Am Coll Cardiol* 1998; 32:2049-2056.
- [53] Weiger M, Pruessmann KP, Boesiger P. Cardiac real-time imaging using SENSE. *Magn Reson Med* 2000;43:177-184.
- [54] Setser RM, Fischer SE, Lorenz CH. Quantification of left ventricular function with magnetic resonance images acquired in real time. *J Magn Reson Imag* 2000;12:430-438.
- [55] Nagel E, Schneider U, Schalla S, et al. Magnetic resonance real-time imaging for the evaluation of left ventricular function. *J Cardiovasc Magn Reson* 2000;2:7-14.
- [56] Guttmann MA, Aletras AH, McVeigh ER. Multi-echo TrueFISP in the heart (abstract). In: Proceedings of the 9th Annual Meeting of the ISMRM, Glasgow 2001: p.110.
- [57] Slavin GS, Foo TK. Cardiac imaging using echo-planar steady-state free precession (abstract). In: Proceedings of the 9th Annual Meeting of the ISMRM, Glasgow 2001: p.443
- [58] Shankaranarayanan A, Simonetti OP, Laub G, et al. Segmented k-space and real-time cardiac cine MR imaging with radial trajectories. *Radiology* 2001;221:827-36.
- [59] Peters DC, McVeigh ER. Ultra-high resolution true FISP projection reconstruction acquisition for cardiac function evaluation (abstract). In: Proceedings of the 9th Annual Meeting of the ISMRM, Glasgow 2001: p.1880.
- [60] Larson AC, Simonetti OP. Real-time cardiac cine imaging with SPIDER: steady-state projection imaging with dynamic echo-train readout. *Magn Reson Med* 2001;46:1059-1066.
- [61] Sodickson DK, Manning WJ. Simultaneous acquisition of spatial harmonics (SMASH): fast imaging with radiofrequency coil arrays. *Magn Reson med* 1997; 38:591-603.
- [62] Madore B, Fredrickson JO, Alley MT, et al. Unaliasing by Fourier-encoding the overlaps using the temporal dimension (UNFOLD), applied to cardiac imaging and fMRI. *Magn Reson Med* 1999; 42:813-828.
- [63] Rehwald WG, Kim RJ, Simonetti OP, et al. Theory of high-speed MR imaging of the human heart with the selective line acquisition mode. *Radiology* 2001; 220:540-547.
- [64] Sanz G, Castaner A, Betriu A, et al. Determinants of prognosis in survivors of myocardial infarction: a prospective clinical angiographic study. *N Engl J Med* 1982; 306:1065-1070.
- [65] Weiss JL, Marino PN, Shapiro EP. Myocardial infarct expansion: recognition, significance and pathology. *Am J Cardiol* 1991; 68:35D-40D.
- [66] Abraham TP, Nishimura RA. Myocardial strain: can we finally measure contractility? *J Am Coll Cardiol* 2001;37:731-734.
- [67] Lieberman AN, Weiss JL, Jugdutt BI, et al. Two-dimensional echocardiography and infarct size: relationship of regional wall motion and thickening to the extent of myocardial infarction in the dog. *Circulation* 1981; 63:739-746.
- [68] Sasayama S, Franklin D, Ross J Jr., et al. Dynamic changes in left ventricular wall thickness and their use in analyzing cardiac function in the conscious dog: a study based on a modified ultrasonic technique. *Am J Cardiol* 1976; 38:870-879.
- [69] Beyar R, Shapiro EP, Graves WL, et al. Quantification and validation of left ventricular wall thickening by a three-dimensional volume element magnetic resonance imaging approach. *Circulation* 1990;81:297-307.
- [70] Buchalter MB, Sims C, Dixon AK, et al. Measurement of regional left ventricular function using labelled magnetic resonance imaging. *Br J Radiol.* 1991;64:953-8.
- [71] Bogaert J, Rademakers FE. Regional nonuniformity of normal adult human left ventricle. *Am J Physiol Heart Circ Physiol.* 2001 Feb;280:H610-20.
- [72] Mirsky I, Parmley WW. Assessment of passive elastic stiffness for isolated heart muscle and the intact heart. *Circ Res* 1973;33:233-243.
- [73] Azhari H, Weiss JL, Rogers WJ, et al. A noninvasive comparative study of myocardial strain in ischemic canine hearts using tagged MRI in 3D. *Am J Phys* 1995; 268:H1918-H1926.
- [74] Götte MJW, van Rossum AC, Twisk JWR, et al. Quantification of regional contractile function after infarction: strain analysis superior to wall thickening analysis in discriminating infarct from remote myocardium. *J Am Coll Cardiol* 2001; 37:808-817.
- [75] McVeigh ER, Zerhouni EA. Noninvasive measurement of transmural gradients in myocardial strain with MR imaging. *Radiology* 1991;180: 677-683.
- [76] Clark NR, Reichek N, Bergey P, et al. Circumferential myocardial shortening in the normal human left ventricle: assessment by magnetic resonance imaging using spatial modulation of magnetization. *Circulation* 1991;84:67-74.
- [77] Mc Veigh ER. MRI of myocardial function: motion tracking techniques. *Magn Reson Imaging* 1996; 14:137-150.
- [78] McVeigh ER, Atalar E. Cardiac tagging with breath-hold cine MRI. *Magn Reson Med* 1992; 28:318-327.
- [79] Stuber M, Spiegel MA, Fischer SE, et al. Single breath-hold slice-following C-SPAMM myocardial tagging. *MAGMA* 1999;9:85-91.
- [80] Buchalter MB, Weiss JL, Rogers WJ, et al. Noninvasive quantification of left ventricular rotational deformation in normal humans using magnetic resonance imaging myocardial tagging. *Circulation* 1990;81:1236-1244.
- [81] Lorenz CH, Pastorek JS, Bundy JM. Delineation of normal human left ventricular twist throughout systole by tagged magnetic resonance imaging. *J Cardiovasc Magn Reson* 2000;2:97-108.
- [82] Osman NF, Kerwin WAS, McVeigh ER, Prince JL. Cardiac motion tracking using CINE harmonic phase (HARP) magnetic resonance imaging. *Magn Reson Med* 1999; 42:1048-1060.
- [83] Garot J, Bluemke DA, Osman NF, et al. Fast determination of regional myocardial strain fields from tagged cardiac images using harmonic phase MRI. *Circulation* 2000; 101:981-988.
- [84] Sampath S, Derbyshire JA, Osman NF, et al. Real-Time imaging of cardiac strain using ultrafast HARP sequence (abstract). In: Proceedings of the 9th Annual Meeting of the ISMRM, Glasgow 2001:111.
- [85] Kraitchman D, Sampath S, Derbyshire J, et al. Detecting the onset of ischemia using real-time HARP (abstract). In: Proceedings of the 9th Annual Meeting of the ISMRM, Glasgow 2001:117.
- [86] Aletras AH, Balaban RS, Wen H. High-resolution strain analysis of the human heart with fast-DENSE. *J Magn Reson.* 1999;140:41-57.
- [87] Braunwald E. Heart disease: A textbook of cardiovascular medicine, 5th edition, 1997. Philadelphia, PA: W.B. Saunders Company, 1997; 288-90.
- [88] Lima JA, Judd RM, Bazille A et al. Regional heterogeneity of human myocardial infarcts demonstrated by contrast-enhanced MRI. Potential mechanisms. *Circulation* 1995;92:1117-1125.
- [89] Wu KC, Zerhouni EA, Judd RM et al. Prognostic significance of microvascular obstruction by magnetic resonance imaging in patients with acute myocardial infarction. *Circulation* 1998;97:765-772.
- [90] Kim RJ, Fieno DS, Parrish TB, Harris K, Chen EL, Simonetti O, Bundy J, Finn JP, Klocke FJ, Judd RM. Relationship of MRI delayed contrast enhancement to irreversible injury, infarct age, and contractile function. *Circulation* 1999; 100 : 1992-2002.
- [91] Haase A. Snapshot FLASH MRI. Applications to T1, T2 and chemical shift imaging. *Magn Reson Med* 1990; 13: 77-89.

- [92] Atkinson DJ, Burstein D, Edelman RR. First-pass cardiac perfusion: evaluation with ultrafast MR imaging. *Radiology* 1990; 174: 757-62.
- [93] Manning WJ, Atkinson DJ, Grossman W, Paulin S, Edelman RR. First pass nuclear magnetic resonance imaging studies using gadolinium-DTPA in patients with coronary artery disease. *J Am Coll Cardiol* 1991; 18: 959-65.
- [94] Wilke N, Simm C, Zhang, Ellermann, Ya X, Merkle, Path G, Lüdemann H, Bache RJ, U_urbil. Contrast-enhanced first pass myocardial perfusion imaging: Correlation between myocardial blood flow in dogs at rest and during hyperemia. *Magn Reson Med* 1999; 41: 100-107.
- [95] Mansfield P. Multiplanar image formation using NMR spin echoes. *J Phys C: Solid State Phys* 1977; 10: L55-8.
- [96] McKinnon GC. Interleaved echo planar phase contrast angiography. *Magn Reson Med* 1994; 32: 682-5.
- [97] Ding S, Wolff SD, Epstein FH. Improved coverage in dynamic contrast-enhanced cardiac MRI using interleaved gradient echo EPI. *Magn Reson Med* 1998; 39: 514-9.
- [98] Bertschinger KM, Nanz D, Buechi M, Luescher TF, Marincek B, von Schulthess GK, Schwitler J. Magnetic resonance myocardial first-pass perfusion imaging: Parameter optimization for signal response and cardiac coverage. *J Magn Reson Imag* 2001; 14: 556-62.
- [99] Schwitler J, Nanz D, Kneifel S, Bertschinger K, Büchi M, Knüsel PR, Marincek B, Lüscher TF, von Schulthess GK. Assessment of myocardial perfusion in coronary artery disease by magnetic resonance. *Circulation* 2001; 103: 2230-5.
- [100] Slavin GS, Wolff SD, Gupta SD, Foo TKF. First-pass myocardial perfusion MR imaging with interleaved notched saturation: Feasibility study. *Radiology* 2001; 219: 258-63.
- [101] Wilke N, Jerosch-Herold M, Wang Y, Huang Y, Christensen BV, Stillman AE, Ugurbil K, McDonald K, Wilson RF. Myocardial perfusion reserve: assessment with multisection, quantitative, first-pass MR imaging. *Radiology* 1997; 204: 373-84.
- [102] Jerosch-Herold M, Wilke N. MR first pass imaging: quantitative assessment of transmural perfusion and collateral flow. *Int J Card Imaging* 1997; 13: 205-18.
- [103] Keijer JT, van Rossum AC, van Eenige MJ, Bax JJ, Visser FC, Teule JJ, Visser CA. Magnetic resonance imaging of regional myocardial perfusion in patients with single-vessel coronary artery disease: quantitative comparison with (201)Thallium-SPECT and coron
- [104] Cullen JH, Horsfield MA, Reek CR, Cherryman GR, Barnett DB, Samani NJ. A myocardial perfusion reserve index in humans using first-pass contrast-enhanced magnetic resonance imaging. *J Am Coll Cardiol* 1999; 33: 1386-94.
- [105] Al-Saadi N, Nagel E, Gross M, Bornstedt A, Schnackenburg B, Klein C, Klimek W, Oswald H, Fleck E. Noninvasive detection of myocardial ischemia from perfusion reserve based on cardiovascular magnetic resonance. *Circulation* 2000; 101: 1379-83.
- [106] Kim RJ, Fieno DS, Parrish TB et al. Relationship of MRI delayed contrast enhancement to irreversible injury, infarct age, and contractile function. *Circulation* 1999;100:1992-2002.
- [107] Rogers WJJ, Kramer CM, Geskin G et al. Early contrast-enhanced MRI predicts late functional recovery after reperfused myocardial infarction [see comments]. *Circulation* 1999;99:744-750.
- [108] Bremerich J, Saeed M, Arheden H et al. Normal and infarcted myocardium: differentiation with cellular uptake of manganese at MR imaging in a rat model. *Radiology* 2000;216:524-530.
- [109] Kim RJ, Judd RM, Chen EL et al. Relationship of elevated 23Na magnetic resonance image intensity to infarct size after acute reperfused myocardial infarction. *Circulation* 1999;100:185-192.
- [110] Simonetti OP, Kim RJ, Fieno DS et al. An improved MR imaging technique for the visualization of myocardial infarction. *Radiology* 2001; 218:215-223.
- [111] Kim RJ, Chen EL, Lima JA et al. Myocardial Gd-DTPA kinetics determine MRI contrast enhancement and reflect the extent and severity of myocardial injury after acute reperfused infarction. *Circulation* 1996;94:3318-3326.
- [112] Rehwald WG, Fieno DS, Chen EL et al. Myocardial magnetic resonance imaging contrast agent concentrations after reversible and irreversible ischemic injury. *Circulation* 2002;105:224-229.
- [113] Klein C, Nekolla SG, Bengel FM et al. Assessment of myocardial viability with contrast-enhanced magnetic resonance imaging: comparison with positron emission tomography. *Circulation* 2002;105:162-167.
- [114] Ricciardi MJ, Wu E, Davidson CJ et al. Visualization of discrete microinfarction after percutaneous coronary intervention associated with mild creatine kinase-MB elevation. *Circulation* 2001;103:2780-2783.
- [115] Wu E, Judd RM, Vargas JD et al. Visualization of presence, location, and transmural extent of healed Q-wave and non-Q-wave myocardial infarction. *Lancet* 2001;357:21-28.
- [116] Kim RJ, Hillenbrand HB, Judd RM. Evaluation of myocardial viability by MRI. *Herz* 2000;25:417-430.
- [117] Kim RJ, Wu E, Rafael A et al. The use of contrast-enhanced magnetic resonance imaging to identify reversible myocardial dysfunction. *N Engl J Med* 2000;343:1445-1453.
- [118] Judd RM, Lugo-Olivieri CH, Arai M et al. Physiological basis of myocardial contrast enhancement in fast magnetic resonance images of 2-day-old reperfused canine infarcts. *Circulation* 1995;92:1902-1910.
- [119] Oshinski JN, Yang Z, Jones JR et al. Imaging time after Gd-DTPA injection is critical in using delayed enhancement to determine infarct size accurately with magnetic resonance imaging. *Circulation* 2001;104:2838-2842.
- [120] Hillenbrand HB, Kim RJ, Parker MA et al. Early assessment of myocardial salvage by contrast-enhanced magnetic resonance imaging. *Circulation* 2000;102:1678-1683.
- [121] Fieno DS, Kim RJ, Chen EL et al. Contrast-enhanced magnetic resonance imaging of myocardium at risk: distinction between reversible and irreversible injury throughout infarct healing. *J Am Coll Cardiol* 2000;36:1985-1991.
- [122] Choi KM, Kim RJ, Gubernikoff G et al. Transmural extent of acute myocardial infarction predicts long-term improvement in contractile function. *Circulation* 2001;104:1101-1107.
- [123] Rochitte CE, Lima JA, Bluemke DA et al. Magnitude and time course of microvascular obstruction and tissue injury after acute myocardial infarction. *Circulation* 1998;98:1006-1014.
- [124] Wu KC, Kim RJ, Bluemke DA et al. Quantification and time course of microvascular obstruction by contrast-enhanced echocardiography and magnetic resonance imaging following acute myocardial infarction and reperfusion. *J Am Coll Cardiol* 1998;32:1756-1764.
- [125] Ito H, Maruyama A, Iwakura K et al. Clinical implications of the 'no reflow' phenomenon. A predictor of complications and left ventricular remodeling in reperfused anterior wall myocardial infarction. *Circulation* 1996;93:223-228.
- [126] Edelman RR, Manning WJ, Burstein D, Paulin S. Coronary arteries: breath-hold MR angiography. *Radiology* 1991;181:641-643.
- [127] Pennell DJ, Keegan J, Firmin DN, Gatehouse PD, Underwood SR, Longmore DB. Magnetic resonance imaging of coronary arteries: technique and preliminary results. *Br Heart J* 1993;70:315-326.
- [128] Manning WJ, Li W, Edelman RR. A preliminary report comparing magnetic resonance coronary angiography with conventional angiography. *N Engl J Med* 1993;328:828-832.
- [129] Duerinckx AJ, Urman MK. Two-dimensional coronary MR angiography: analysis of initial clinical results. *Radiology* 1994;193:731-738.
- [130] Pennell DJ, Bogren HG, Keegan J, Firmin DN, Underwood SR. Assessment of coronary artery stenosis by magnetic resonance imaging. *Heart* 1996;75:127-133.
- [131] Meyer CH, Hu BS, Nishimura DG, Macovski A. Fast spiral coronary artery imaging. *Magn Reson Med* 1992;28:202-213.
- [132] Taylor AM, Keegan J, Jhooti P, Gatehouse PD, Firmin DN, Pennell DJ. A comparison between segmented k-space FLASH and interleaved spiral MR coronary angiography sequences. *J Magn Reson Imaging* 2000; 11: 394-400.
- [133] Duerinckx A, Atkinson DP. Coronary MR angiography during peak systole: work in progress. *J Magn Reson Imaging* 1997;7:979-986.
- [134] Sakuma H, Caputo GR, Steffens JC, et al. Breath-hold MR cine angiography of coronary arteries in healthy volunteers: value of multiangle oblique imaging planes. *AJR Am J Roentgenol* 1993;188:377-380.
- [135] Foo TKF, Ho VB, Hood MN. Vessel-tracking: prospective adjustment of section-selective MR angiographic locations for improved coronary artery visualization over the cardiac cycle. *Radiology* 2000; 214:283-289.
- [136] Saranathan M, Ho VB, Hood MN, Foo TKF, Hardy CJ. Adaptive Vessel Tracking: Automated Computation of Vessel Trajectories for Improved Efficiency in 2D Coronary MR Angiography. *J Magn Reson Imaging* 2001;14:368-373.
- [137] Duerinckx AJ, Atkinson DP, Minotorovitch J, Simonetti OP, Vrman MK. Two-dimensional coronary MRA: limitations and artifacts. *Eur Radiol* 1996;6:312-325.
- [138] Wang Y, Christy PS, Korosec FR, Alley MT, Grist TM, Polzin JA, Mistretta CA. Coronary MRI with respiratory feedback monitor: the 2D imaging case. *Magn Reson Med* 1995;33:116-121.
- [139] Taylor AM, Keegan J, Jhooti P, Gatehouse PD, Firmin DN, Pennell DJ. Differences between normal subjects and patients with coronary artery disease for three different MR coronary angiography respiratory suppression techniques. *J Magn Reson Imaging* 1999;9:7
- [140] Holland AE, Goldfarb JW, Edelman RR. Diaphragmatic and cardiac motion during

suspended breathing: preliminary experience and implications for breath-hold MR imaging. *Radiology* 1998;209:483-489.

[141] Ehman RL, Felmlee JP. Adaptive technique for high-definition MR imaging of moving structures. *Radiology* 1989;173:255-263.

[142] Li D, Kaushikkar S, Haacke EM, et al. Coronary arteries: three-dimensional MR imaging with retrospective respiratory gating. *Radiology* 1996;201:857-863.

[143] Oshinski JN, Hofland L, Mukundan S Jr, Dixon WT, Parks WJ, Pettigrew RI. Two-dimensional coronary MR angiography without breath holding. *Radiology* 1996;201:737-743.

[144] Post JC, van Rossum AC, Hofman MB, Valk J, Visser CA. Three-dimensional respiratory-gated MR angiography of coronary arteries: comparison with conventional coronary angiography. *AJR Am J Roentgenol* 1996;166:1399-1404.

[145] Wang Y, Rossmann PJ, Grimm RC, Riederer SJ, Ehman RL. Navigator-echo-based real-time respiratory gating and triggering for reduction of respiration effects in three-dimensional coronary MR angiography. *Radiology* 1996;198:55-60.

[146] Taylor AM, Jhooti P, Wiesmann F, Keegan J, Firmin DN, Pennell DJ. MR navigator-echo monitoring of temporal changes in diaphragm position: implications for MR coronary angiography. *J Magn Reson Imaging* 1997;7:629-636.

[147] McConnell MV, Khasgiwala VC, Savord BJ, Chen MH, Chuang ML, Edelman RR, Manning WJ. Comparison of respiratory suppression methods

and navigator locations for MR coronary angiography. *AJR Am J Roentgenol* 1997;168:1369-1975.

[148] Müller MF, Fleisch M, Kroeker R, Chatterjee T, Meier B, Vock P. Proximal coronary artery stenosis: three-dimensional MRI with fat saturation and navigator echo. *J Magn Reson Imaging* 1997;7: 644-651.

[149] Danias PG, McConnell MV, Khasgiwala VC, Chuang ML, Edelman RR, Manning WJ. Prospective navigator correction of image position for coronary MR angiography. *Radiology* 1997;203: 733-736.

[150] Woodard PK, Li D, Haacke EM, et al. Detection of coronary stenoses on source and projection images using three-dimensional MR angiography with retrospective respiratory gating: preliminary experience. *AJR Am J Roentgenol* 1998;170:883-888.

[151] Huber A, Nikolaou K, Gonschior P, Knez A, Stehling M, Reiser M. Navigator echo-based respiratory gating for three dimensional MR coronary angiography: results from healthy volunteers and patients with proximal coronary artery stenoses. *AJR Am J Roentgenol*

[152] Sandstede JJW, Pabst T, Beer M, Geis N, Kenn W, Neubauer S, Hahn D. Three-dimensional MR coronary angiography using the navigator technique compared with conventional coronary angiography. *AJR Am J Roentgenol* 1999;172: 135-139.

[153] Hofman MBM, Paschal CB, Li D, Haacke EM, van Rossum AC, Sprenger M. MRI of coronary arteries: 2D breath-hold vs. 3D respiratory-gated

acquisition. *J Comput Assist Tomogr* 1995;19:56-62.

[154] Foo TKF, Saranathan M, Hardy CJ, Ho VB. Coronary Artery Magnetic Resonance Imaging: A Patient-Tailored Approach. *Top Magn Reson Imaging* 2000;11:406-416.

[155] Brittain JH, Hu BS, Wright GA, Meyer CH, Macovski A, Nishimura DG. Coronary angiography with magnetization-prepared T2 contrast. *Magn Reson Med* 1995;33:689-696.

[156] Botnar RM, Stuber M, Danias PG, Kissinger KV, Manning WJ. Improved coronary artery definition with T2-weighted, free-breathing, three dimensional coronary MRA. *Circulation* 1999;99: 3139-3148.

[157] Kim WY, Danias PG, Stuber M, et al. Coronary magnetic resonance angiography for the detection of coronary stenoses. *N Engl J Med* 2001;345:1863-1869.

[158] Deshpande VS, Shea SM, Laub G, Simonetti OP, Finn JP, Li D. 3D magnetization-prepared True-FISP: a new technique for imaging coronary arteries. *Magn Reson Med* 2001;46:494-502.

[159] Li D, Zheng J, Bae KT, Woodard PK, Haacke EM. Contrast-enhanced magnetic resonance imaging of the coronary arteries. A review. *Invest Radiol* 1998;33:578-586.

[160] Goldfarb JW, Edelman RR. Coronary arteries: Breath-hold, Gadolinium-enhanced, three-dimensional MR angiography. *Radiology* 1998; 206:830-834.

[161] Kessler W, Laub G, Achenbach S, Ropers D, Moshage W, Daniel WG. Coronary arteries: MR